ISSN (Online) 2287-3406
Journal of Life Science **2024** Vol. 34. No. 9. 609~619 DOI : https://doi.org/10.5352/JLS.2024.34.9.609

Enhancement of Protein Aggregate Clearance in Huntington's Disease Model via CRISPR/dCas9 Activation of *NAGK* and *Reln* Genes

Diyah Fatimah Oktaviani[1], Raju Dash[1,2], Sarmin Ummey Habiba[1], Ho Jin Choi[1,3], Yeasmin Akter Munni[1], Dae-Hyun Seog[4], Maria Dyah Nur Meinita[5] and Il Soo Moon[1]*

[1]*Department of Anatomy, College of Medicine, Dongguk University, Gyeongju 38066, Korea*
[2]*Department of New Biology, Daegu Gyeongbuk Institute of Science and Technology, Daegu 42988, Korea*
[3]*Medical Institute of Dongguk University Gyeongju 38066, Korea*
[4]*Department of Biochemistry, Dementia and Neurodegenerative Disease Research Center, Inje University College of Medicine, Busan 47392, Korea*
[5]*Faculty of Fisheries and Marine Science, Jenderal Soedirman University, Purwokerto 53122, Indonesia*

Received August 2, 2024 /Revised August 7, 2024 /Accepted September 3, 2024

Neurodegenerative diseases are marked by the accumulation of toxic misfolded proteins in neurons. Therefore, strategies for the effective prevention and clearance of aggregates are crucial for therapeutic interventions. Cytoplasmic dynein plays a crucial role in the clearance of aggregates by transporting them to the cell center, where lysosomes are enriched and the aggregates undergo extensive autophagic degradation. Previously, we reported evidence for the activation of dynein by N-acetylglucosamine kinase (NAGK) and Reln. In the present study, we explored the effects of NAGK and Reln upregulation on the clearance of aggregates. To upregulate *NAGK* and *Reln* genes in HEK293T cells (a human embryonic kidney cell line), CRISPR/dCas9 activation systems (CASs) were used with specific plasmids encoding target-specific 20 nt guide RNA. The effects of this genetic modulation were analyzed in Huntington's disease cellular models, including HEK293T cells and primary mouse cortical cells, where external mutant huntingtin (mHtt, Q74) aggregates were induced. The results showed that the CAS activation of *NAGK* or *Reln*, or their combination, significantly reduced the proportion of cells with Q74 aggregates (aggresomes). This effect was reversed by Ciliobrevin D (a dynein inhibitor) and chloroquine (an autophagy inhibitor), indicating the role of dynein-mediated autophagy in aggregate clearance. These findings provide the basis for therapeutic strategies aimed at enhancing neuronal health through targeted gene activation.

Key words : CRISPR/dCas9 activation system, mHtt, NAGK, neuron, Reln

Introduction

Neurodegenerative disorders (NDs) are often referred to as "proteinopathies", or "protein misfolding diseases", because their pathogenesis involves protein misfolding and aggregation [15, 46]. Huntington's disease (HD) is one such proteinopathy, where the disease occurs due to the accumulation of mutant huntingtin (mHtt) protein aggregates. The mHtt aggregation is caused by the polyglutamine expansion in the protein, which is, in turn, due to a mutation in the gene. In HD, the CAG repeat expands in exon 1 of the IT-15 ("interesting transcript 15") gene encoding the huntingtin protein [8]. Up to 35 CAG repeats are considered within the range of normal variation, while 36 or more repeats are abnormal and associated with selective neuronal death, occurring mainly in the cerebral cortex and the striatum, eventually causing the brain to become smaller than normal [45].

In eukaryotes, there are two main mechanistic pathways for proteolysis: the ubiquitin-proteasome system (UPS) and the autophagy-lysosomal pathway (ALP) [2, 13, 23, 31]. It is believed that short-lived intracellular proteins are mainly removed by the UPS, while long-lived proteins, misfolded proteins, protein aggregates, and damaged organelles are degraded by the ALP [23]. Aggregated proteins like mHtt are inefficiently degraded by the proteasome due to their large size. Therefore, autophagy is the main pathway to effectively degrade aggregate-prone proteins like mHtt [27].

***Corresponding author**
Tel : +82-54-770-2414, Fax : +82-54-770-2447
E-mail : moonis@dongguk.ac.kr

As a cytoskeletal motor, dynein might play an important role in the initial response to protein aggregation due to its function in endosomal and lysosomal transport [6]. Dynein plays a crucial role in autophagosome-lysosome fusion in the ALP [46]. Misfolded protein aggregates like mutant alpha-synuclein and mHtt are transported to the microtubule organizing center (MTOC) by dynein retrograde transport, where they fuse with lysosomes and are cleared by the ALP [11, 22, 38]. Indeed, autophagosome fusion with lysosomes is disrupted when dynein function is impaired [46]. The number of protein aggregates increases and they remain dispersed in the cytoplasm during genetic repression of dynein [9], indicating that dynein function is critical and essential for the clearance of protein aggregates.

Therefore, it is a reasonable hypothesis that activation of dynein transport may accelerate the clearance of mHtt aggregates. One signaling molecule targeting the activation of dynein is Reln, a product of the *Reln* gene. Upregulation of Reln signaling promotes neuronal migration [16] suggesting dynein activation. Binding of Reln to its receptors, very low-density lipoprotein receptor (VLDLR) and apolipoprotein E receptor 2 (apoER2), induces Disabled-1 (Dab1) tyrosine phosphorylation, which acts as a hub to recruit different downstream SH2 domain-containing proteins including Lis1 (reviewed in [14]). LIS1 is known to function as a microtubule (MT) and MTOC-associated protein that regulates nucleokinesis along MTs via the regulation of dynein motor function [44]. LIS1 forms a complex including NDEL1 (NudE isoform, NudE-like), which directly binds dynein [34].

Another protein targeting the activation of dynein is *N*-acetylglucosamine kinase (NAGK). In our previous report, we showed that NAGK promotes dynein activation by interacting with dynein light chain roadblock type 1 (DYNLRB1) [18, 19, 39]. These interactions promote the clearance of mHtt (Q74) aggregates with polyglutamine expansion [39], nuclear invagination during cell division, cell migration [19], cell division [40], dendritic branch point & branching [19]. Therefore, activation of the *NAGK* and *Reln* genes is reasonably considered to accelerate the clearance of protein aggregates.

Recently, an exciting new genome editing technology called the CRISPR/Cas9 system has been revealed. Clustered regularly interspaced short palindromic repeats (CRISPR) and the CRISPR-associated protein 9 (Cas9) system can be used to effectively modify genes with the help of specific guide RNA (gRNA) [37]. It has been developed to activate the expression of endogenous genes by targeting a fusion protein of deactivated Cas9 (dCas9) and a transactivation domain to synergistic activation mediators (SAM) via different combinations of gRNAs [36]. This new system can be used to activate transcription factors at the normal physiological site of the nucleus [37]. In the present study, we took advantage of the CAS system to activate the *NAGK* and *Reln* genes and investigated the clearance effects of mHtt aggregates in cellular models of HD.

Materials and Methods

HEK293T cell culture

HEK293T cells were cultured in 24 well plates containing Dulbecco's modified Eagle's medium (DMEM) supplemented with 10% fetal bovine serum (FBS) and 1% penicillin streptomycin up to 60–70% confluency. Cells were incubated at 37°C under 5% CO_2 and 95% air.

Neuronal culture

Cortical cells were prepared from mouse embryonic fetuses at 17 days of gestation (E17). A time-pregnant (14th day of gestation) ICR mouse was purchased from Koatech (Pyeongtaek, Korea) and housed in controlled temperature with access to food and water *ad libitum*. After 3 days, the pregnant mouse was euthanized with isoflurane and the fetuses were collected. All procedures were approved by the Institution Animal Care and Use Committee of Dongguk University (approval certificate number IUCAC-2018-06). The cerebral cortices were dissected from the brain and dissociated neuronal cultures were prepared as previously described with some modification [4]. Briefly, the dissected cerebral cortices were collected in Hank's balanced salt solution (HBSS), and the tissues were dissociated by trypsinization (0.25% trypsin in HBSS) for 14 min at 37°C, and triturated with fire-polished graded Pasteur pipettes. The dissociated cells were seeded onto poly-DL-lysine (Sigma-Aldrich, St. Louis, MO, USA) coated 12-mm glass coverslips in 24-well culture plates at a density of 5.0×10^4 cells/cm^2. Cells were seeded in 2-days preincubated plating media (serum-free neurobasal media supplemented with B27, glutamate and β-mercaptoethanol) and incubated at 37°C under 5% CO_2 and 95% air.

Transfection of *NAGK* and *Reln* CRISPR/dCas9 activation system

To upregulate *NAGK* and *Reln* genes in HEK293T cell (a human embryonic kidney cell line), CRISPR/dCas9 activation systems (CASs) were used (Santa Cruz Biotechnology, Dallas, TX, USA). The CAS plasmids are a synergistic activation

mediator (SAM) transcription activation system designed to specifically upregulate gene expression, and consist of the following three plasmids at a 1:1:1 mass ratio: a plasmid encoding the deactivated Cas9 (dCas9) nuclease (D10A and N863A) fused to the transactivation domain VP64; a plasmid encoding the MS2-p65-HSF1 fusion protein; and a plasmid encoding a target-specific 20 nt guide RNA. For target-specific 20 nt guide RNAs, we used *NAGK* (sc-407809-ACT-2; Santa Cruz Biotechnology), *Reln* (sc-401862-ACT-2; Santa Cruz) and control CAS plasmids (sc-437275; Santa Cruz Biotechnology). CAS plasmids were transfected into HEK 293T cells using plasmid transfection medium and Ultra Cruz transfection reagent (Santa Cruz Biotechnology) according to the manufacturer's protocol. Briefly, cells (1×10^5 cells per well) were seeded on 24-well culture plates in antibiotic-free DMEM 24 hr before transfection and grown to 70% confluence. Cells were transfected with 1.0 μg CAS plasmid using Ultra Cruz Transfection Reagents and incubated in cell culture incubator (37°C, 5% CO_2/95% air). The transfection efficiencies of all plasmids ranged from 70 to 80%.

Immunocytochemistry

Cells on coverslip were fixed consecutively with paraformaldehyde and methanol [32]. Briefly, coverslips were incubated in 4% paraformaldehyde in Phosphate-buffered saline (PBS) at room temperature (RT) for 15 min, followed by methanol fixation at -20°C for 20 min. Fixed cells were then blocked using 5% normal goat serum, 0.05% Triton X-100 in PBS, pH 7.4 for 1 hr at RT. Primary antibodies were added to coverslip and incubated overnight at 4°C. Subsequently, the coverslips were rinsed with blocking buffer, then incubated with fluorophore-labelled secondary antibodies at RT for 1.5 hr. Coverslips were sequentially rinsed with blocking buffer and PBS, and mounted on glass slides. The following antibodies were used for immunostaining including tubulin α-subunit (mouse monoclonal 12G10, 1:1,000 dilution; Developmental Studies Hybridoma Bank, University of Iowa, Iowa City, IA, USA), rabbit polyclonal NAGK (1:200; Genetex, Irvine, CA, USA); rabbit polyclonal Reln (1:100; GeneTex). The fluorescently labeled secondary antibodies Alexa Fluor 488-conjugated goat antimouse IgG and Alexa Flour 568-conjugated goat antirabbit IgG were from Invitrogen (Thermo Fisher Scientific, Carlsbad, CA, USA).

Western blots

At 24 hr incubation after transfection, cells were washed with cold PBS and lysed in lysis buffer (25 mM Tris, 150 mM NaCl, 1.0 mM EDTA, 1% NP-40, 5% glycerol; pH 7.4) containing protease inhibitor cocktail (Thermo Fisher Scientific). Equal amounts of proteins were electrophoresed on 8% sodium dodecyl sulfate (SDS)-polyacrylamide or 15% Tricine-SDS-PAGE, and transferred to polyvinylidene fluoride (PVDF) membranes. Membranes were incubated overnight at 4°C with primary antibodies (tubulin β-subunit (mouse monoclonal 12G10, 1:1,000; Developmental Studies Hybridoma Bank), microtubule associated protein 1 light chain 3 (rabbit polyclonal LC3, 1:1,000; Cell Signaling Technology, Danvers, MA, USA), α-actin (mouse monoclonal JLA20, 1:1,000; Developmental Studies Hybridoma Bank), Ubiquitin (mouse monoclonal, 1:1,000; Santa Cruz Biotechnology), Sequestosome-1/P62 (SQSTM1 mouse monoclonal, 1:1,000; Proteintech Group, Chicago, IL, USA) and GFP Antibody (PA1-980A, 1:1,000; Invitrogen, Waltham, MA, USA)). After rinsing with TTBS (0.05% Tween-20 in TBS), membranes were incubated with horse radish peroxidase-conjugated secondary antibodies (1:1,000; anti-mouse or anti-rabbit IgG; Amersham Biosciences, now GE Healthcare Life Sciences, Middlesex County, NJ, USA). The blots were detected using an ECL detection kit (Abfrontier, Seoul, Korea). To strip membranes, stripping buffer was used (LPS Solution, Daejeon, Korea).

Measurement of GFP-tagged mutant huntingtin (Q74) aggregates

HEK293T and brain cortical cells were transiently co-transfected with GFP-tagged mutant huntingtin plasmid Q74 (pEGFP-Q74) which contains human HTT partial exon 1 Q74 (a gift from David Rubinsztein (Addgene plasmid #40262; http://n2t.net/addgene:40262; RRID:Addgene 40262)) [33] with each CAS plasmids using plasmid transfection medium and Ultra Cruz transfection reagent (Santa Cruz Biotechnology) according to the manufacturer's protocol. Cells were observed under a fluorescence (Leica Microsystems AG, Wetzlar, Germany) at 2× magnification at 24 to 48 hr after transfection. The fluorescence intensity, size and number of GFP-positive aggregates in HEK293T and brain cortical cells were analyzed using Image J software (version 1.45, National Institute of Health, Bethesda, MD, USA). In some experiments ciliobrevin D (20 μM) and an autophagy blocker chloroquine (CQ, 50 μM) was used to block cytoplasmic dynein and the autophagy, respectively. In these cases, the inhibitor was added to cultures after 6 hr of transfection, and cells were observed after further incubation for 18 hr.

Image acquisition

Phase contrast and fluorescence images (1,388×1,039 pixels) were acquired from a Leica Research Microscope DM IRE2 (Leica Microsystems AG). The density quantification was performed using an ImageJ Fiji program [39]. Image contrast, clarity and brightness were adjusted using Adobe Systems Photoshop 7.0 software (Adobe, San Jose, CA, USA).

Statistics

All results are presented as mean ± SEM (standard error of the mean). The Student's *t*-test was used to compare two groups, and one-way ANOVA with Duncan's multiple comparison *post hoc* test was used for multi-group comparisons. p values of <0.05 were deemed statistically significant, and p values of <0.001 were considered very significant. Statistical analysis was performed using GraphPad Prism v 8.0 (GraphPad Software, San Diego, CA, USA).

Results

Overexpression of *NAGK* and *Reln* genes using CRISPR/dCAS9 activation system (CAS) *in vitro*

Using CAS system, we induced upregulation of *NAGK* and *Reln* genes, which is expected to promote dynein function. As a first step we confirmed the upregulation of these genes by assessing the levels of expressed proteins in HEK293T cells. Cells were transfected with CAS plasmids and immunostained after 24 hr incubation using rabbit anti-NAGK and anti-Reln antibodies. As shown in Fig. 1A the expression levels of NAGK and Reln were significantly increased in the cytoplasm of the cells compared to the cells transfected with control CAS plasmids. Statistical analyses showed the increases were very significant (p<0.001) (Fig. 1B).

Using CAS system, we induced upregulation of *NAGK* and *Reln* genes, which is expected to promote dynein function. As a first step we confirmed the upregulation of these genes by assessing the levels of expressed proteins in HEK293T cells. Cells were transfected with CAS plasmids and immunostained after 24 hr incubation using rabbit anti-NAGK and anti-Reln antibodies. As shown in Fig. 1A the expression levels of NAGK and Reln were significantly increased in the cytoplasm of the cells compared to the cells transfected with control CAS plasmids. Statistical analyses showed the increases were very significant (p<0.001) (Fig. 1B).

Upregulation NAGK and Reln reduces accumulation of Q74-mHtt aggregates in HEK293 cells: synergistic effects

Having confirmed the upregulation of NAGK and Reln expression by CAS, we next assessed the effect of their upregulation on the clearance of mHtt aggregates. NAGK and Reln activate dynein motor through different mechanism (see Discussion). To explore whether activation of the two genes by CAS promotes Q74 aggregate clearance, we co-transfected HEK293T cells with pEGFP-mHtt (pQ74) and CAS plasmids. Live cell images were observed at 24 hr after transfection, and cells were fixed and stained at 48 hr after transfection with anti-GFP antibody to reveal Q74 aggregates. Representative fluorescence images were shown in Fig. 2A, and stat-

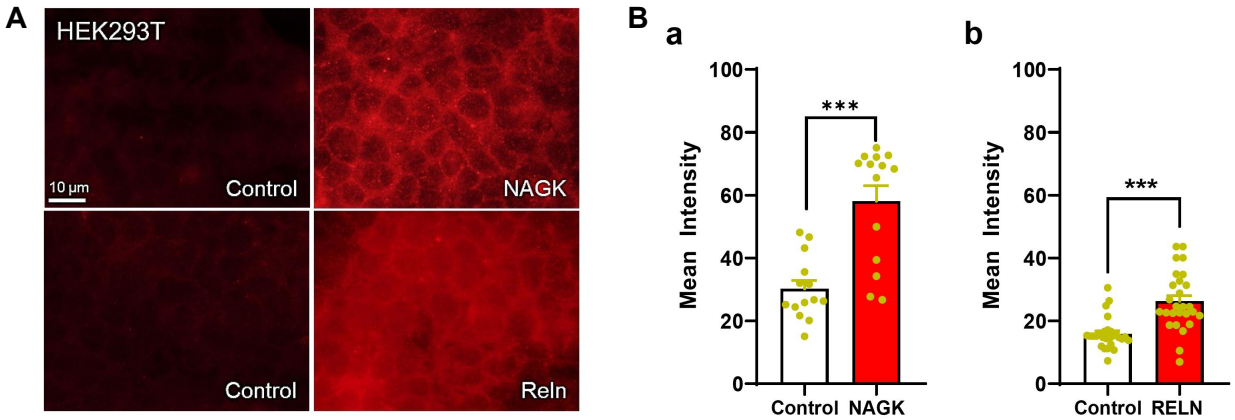

Fig. 1. Upregulation of NAGK and Reln by CRISPR/dCas9 System. Expression levels of NAGK and Reln were assessed using immunofluorescence staining. HEK293T cells were transfected with Control, *NAGK* and *Reln* CRISPR activation plasmids. (A) After 24 hr of incubation, cells were fixed and stained with indicated antibodies. (B) The level of NAGK and Reln expression were shown by mean fluorescence intensity (a.u., arbitrary unit). ***p<0.001. Scale bar, 10 μm.

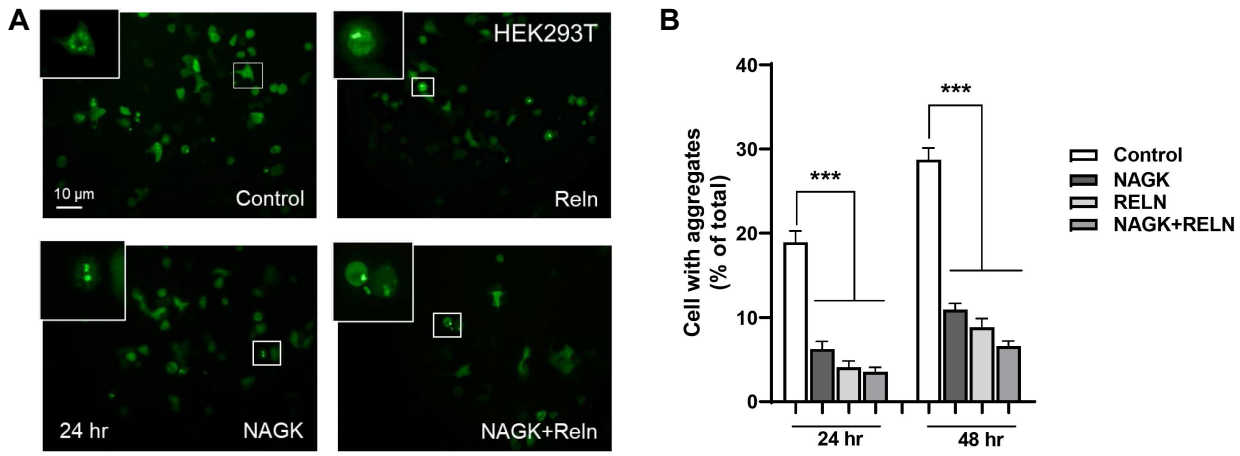

Fig. 2. Effect of *NAGK* and *Reln* CAS activation reduced the portion of HEK293T cells containing mHtt aggregates in cellular HD models. HEK293T cells were co-transfected with pEGFP-mHtt (pQ74) and indicated CAS plasmids. After 48 hr of incubation, cells with aggregates were counted and expressed as percentages of total cell counts (n=500). Note that the portions of aggregate-containing cells were very significantly (p<0.001) reduced in gene-activated groups compared with control. ***p<0.001. Scale bar, 50 μm.

istical analyses showed that the portions of cells containing mHtt aggregates were very significantly (p<0.001) reduced in both *NAGK* and *Reln* CAS-activated groups compared with control CAS one (Fig. 2B) at both 24 and 48 hr after transfection, indicating that *NAGK* and *Reln* CAS activation promoted clearance of Q74-mHtt aggregates. In addition, cells containing Q74 aggregates were more significantly reduced when both NAGK and Reln are upregulated (Fig. 2B, NAGK-Reln), indicating a synergistic effect.

Synergistic effects of *NAGK* and *Reln* CAS on Q74 clearance in cortical neurons

Similar effects as in HEK293 cells were also manifested in neurons. Cultured rat brain cortical cells were co-transfected. After 24 hr of transfection, live cell images were observed under fluorescence microscope (Fig. 3A). After 48 hr of transfection, cells were fixed and double-labeled with anti-β tubulin and anti-GFP, and counter-stained with DAPI (Fig. 3A). Statistical analyses revealed that the portion of cells containing Q74 aggregates was significantly (p<0.01) reduced in single CAS transfected neurons (Fig. 3B). In addition, cells transfected with combined *NAGK* and *Reln* CAS plasmids showed very significant reduction (p<0.001), compared to control CAS transfected neurons (Fig. 3B, NAGK + Reln). These results indicate synergistic effects of NAGK and Reln on Q74 clearance in neurons.

Role of autophagy in the clearance of Q74 aggregates in *NAGK* and *Reln* upregulation

Unfolded proteins first form small soluble aggregates throughout cytoplasm. These soluble aggregates are transported by dynein motor to the cell center and form large insoluble aggregates, which in turn form aggresomes [21]. Autophagy may be responsible for the clearance of the Q74 aggresomes. To confirm this hypothesis, we fractionated Q74 into soluble and insoluble fractions by centrifugation (15 min, 15,000× g at 4°C) and the fractions were subjected to immunoblotting. As shown in Fig. 4A and 4B the levels of soluble and insoluble Q74 were significantly (p<0.01) decreased in *NAGK* and *Reln* CAS transfected cells, indicating that autophagy is activated. To prove activation of autophagy the same Western blots were stripped off and subjected to immunoblotting with autophagic marker proteins. As shown in Fig. 4C, the expression level of p62/SQSTM1 was very significantly (p<0.001) reduced, whereas the type II form of microtubule-associated protein 1 light chain 3 (LC3-II) was very significantly (p<0.001) increased in both *NAGK* and *Reln* CAS activation (Fig. 4D), indicating formation of autophagosome and autophagy degradation of Q74 insoluble aggregates.

Since p62/SQSTM1 also bind to ubiquitylated proteins, in addition to LC3 on autophagosomes form [3], we also investigated the expression level of ubiquitin proteins. As shown in Fig. 4E, the expression level of ubiquitin was also very significantly (p<0.001) decreased confirming activation of autophagy. These results indicate the important role of autophagy in the clearance of polyglutamine disease proteins, which can be reduced by accelerating dynein function through overexpression of NAGK and Reln.

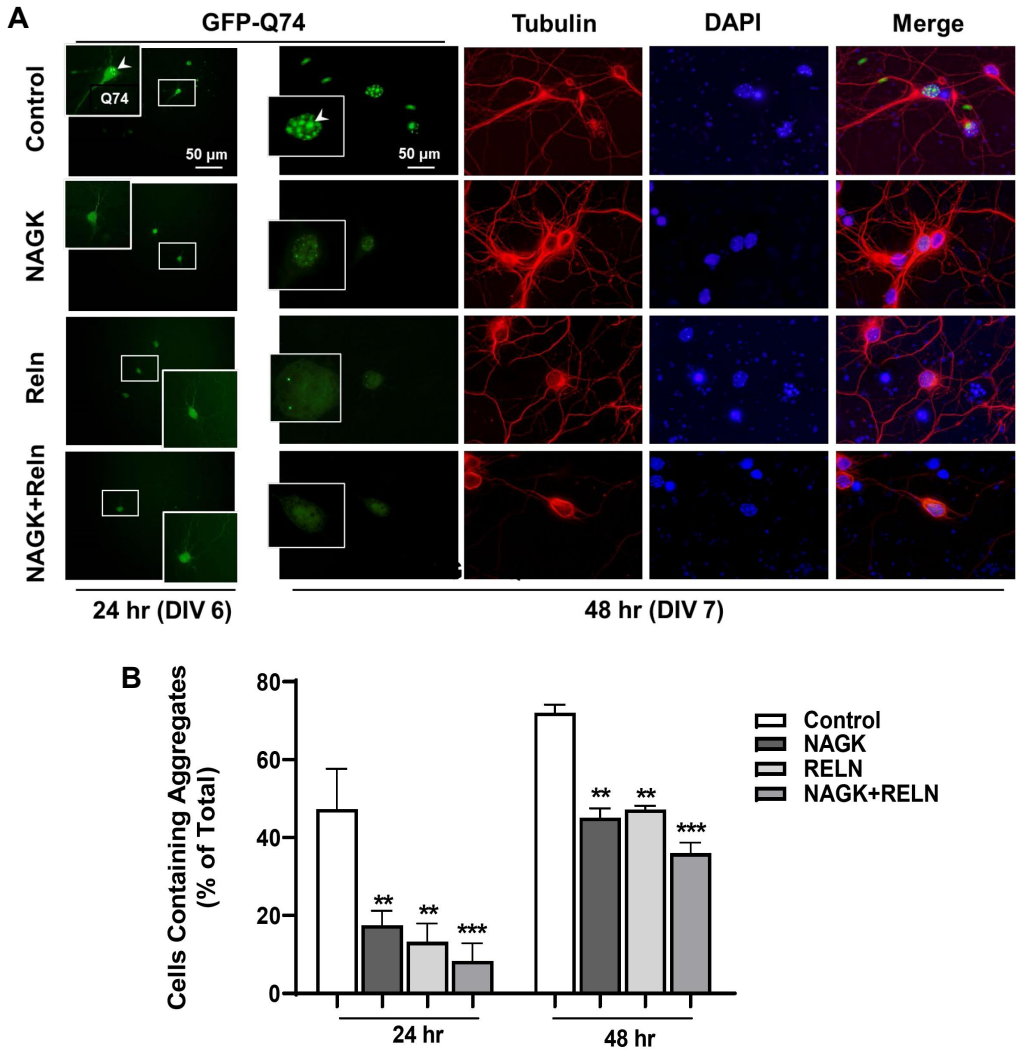

Fig. 3. Synergistic effects of *NAGK* and *Reln* CAS activation on Q74 clearance in a HD model of cortical neurons. Rat cortical cultures were co-transfected with pQ74 and single or combination of *NAGK* and *Reln* CAS plasmids. (A) Typical live fluorescence images after 24 and 48 hr of incubation after transfection. The 24 hr incubated cultures were double-immunostained with indicated antibodies and counter-stained with DAPI. (B) Aggregates-containing cells were counted and expressed as percentages of total cell counts (n=500) $^{**}p<0.01$, $^{***}p<0.001$. Scale bar, 50 μm.

Impairment of dynein function leads to failure of Q74 clearance

Previous reports from our laboratory indicated that NAGK activates dynein [39], and Reln also upregulates dynein expression [16]. Therefore, we assume that the promotion of Q74 clearance by the upregulation of NAGK and Reln is due to the accelerated transport of Q74 clusters by dynein to the cell center, where they form aggresomes that eventually fuse with lysosomes. To prove this assumption we used Ciliobrevin D (a cell-permeable, reversible and specific inhibitor of AAA + ATPase motor cytoplasmic dynein) and CQ, which blocks the autophagic flux by impairing autophagosome-lysosome fusion [28]. Ciliobrevin D (20 μM) and CQ (50 μM) were added to the HEK293T culture medium after 6 hr transfection and further incubated for 24 hr. Typical live cell images were shown in Fig. 5A. Statistical analyses revealed that the portions of Q74 aggregate-containing cells were dramatically increased in both CQ and ciliobrevin D treated cells (Fig. 5B) transfected with single or combined *NAGK* and *Reln* CAS plasmids, with synergistic effects in the latter. These data prove our assumption that NAGK and Reln accelerate intracellular transport of the disease proteins by dynein, formation of aggresomes, and eventual clearance by autophagy.

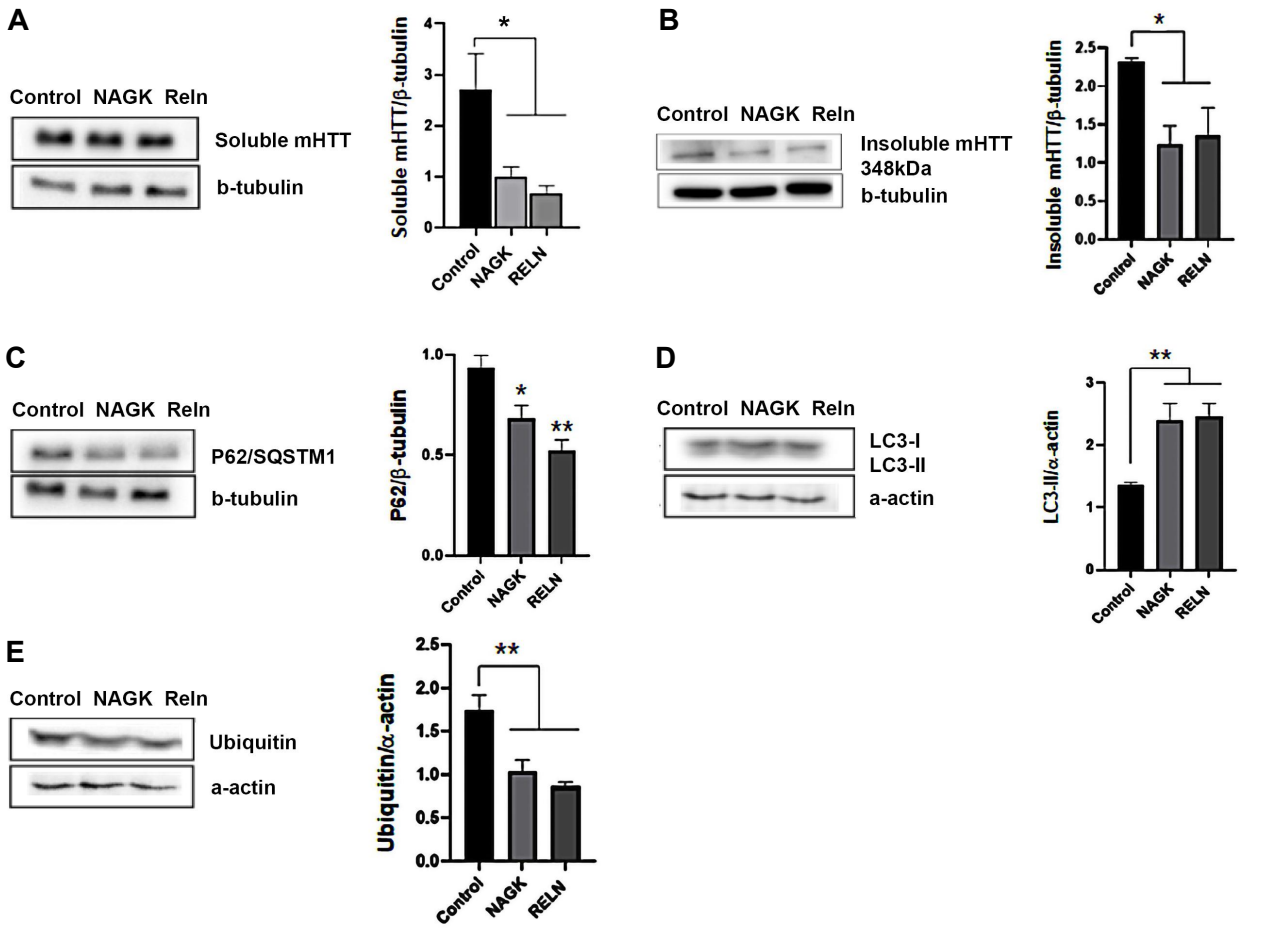

Fig. 4. Autophagy is responsible for the clearance of Q74 aggregates in *NAGK* and *Reln* CAS activation. Blots were probed with the indicated antibody to detect mHtt (pQ74) soluble form (A), mHtt (pQ74) insoluble form (B), autophagy related markers P62/SQSTM1 (C), LC3 (D), and ubiquitin (E). Band intensities were measured and normalized to control blots (tubulin or actin). Statistical significance was determined using one-way ANOVA *p<0.01, **p<0.001.

DISCUSSION

In this present study, we have shown that upregulation of *NAGK* and *Reln* genes by CAS activation induced significant reduction of Q74-mHtt aggregate formation in both HEK293T and cortical neurons. The combination of the two genes resulted in more significant reduction compared to single activation, indicating a synergetic effect. When dynein is inhibited by Ciliobrevin D and CQ (autophagy inhibitor), the clearance effects were erased indicating that this effect stems from activation of dynein.

Neurodegenerative diseases (NDs) are characterized by the accumulation of toxic proteins, caused by an imbalance between production and clearance in the central nervous system (CNS). For example, using metabolic labeling, [29] measured Aβ42 and Aβ40 production and clearance rates in the CNS of participants with Alzheimer's disease (AD) and cognitively normal controls, finding that clearance rates for both Aβ42 and Aβ40 were impaired in AD compared to controls. This indicates that the common late-onset form of AD is characterized by an overall impairment in Aβ clearance. Therefore, although numerous factors contribute to the production of impaired proteins, effective clearance of their accumulation emerges as an attractive therapeutic strategy for NDs.

Mutant proteins such as β-amyloid (Aβ), α-synuclein, and mHtt, which are associated with AD, PD, and HD, respectively, are aggregate-prone, forming small, diffuse 'soluble' aggregates in the cytoplasm. These 'soluble' aggregates are transported by cytoplasmic dynein to the MTOC, where they aggregate to form a large 'aggresome' that fuses with lysosomes to undergo aggrephagy. Aggrephagy is the selective degradation of protein aggregates by autophagy [35]. Therefore, accelerated transportation of 'soluble' aggregates to the MTOC could be a strategy for efficient clearance of cytoplas-

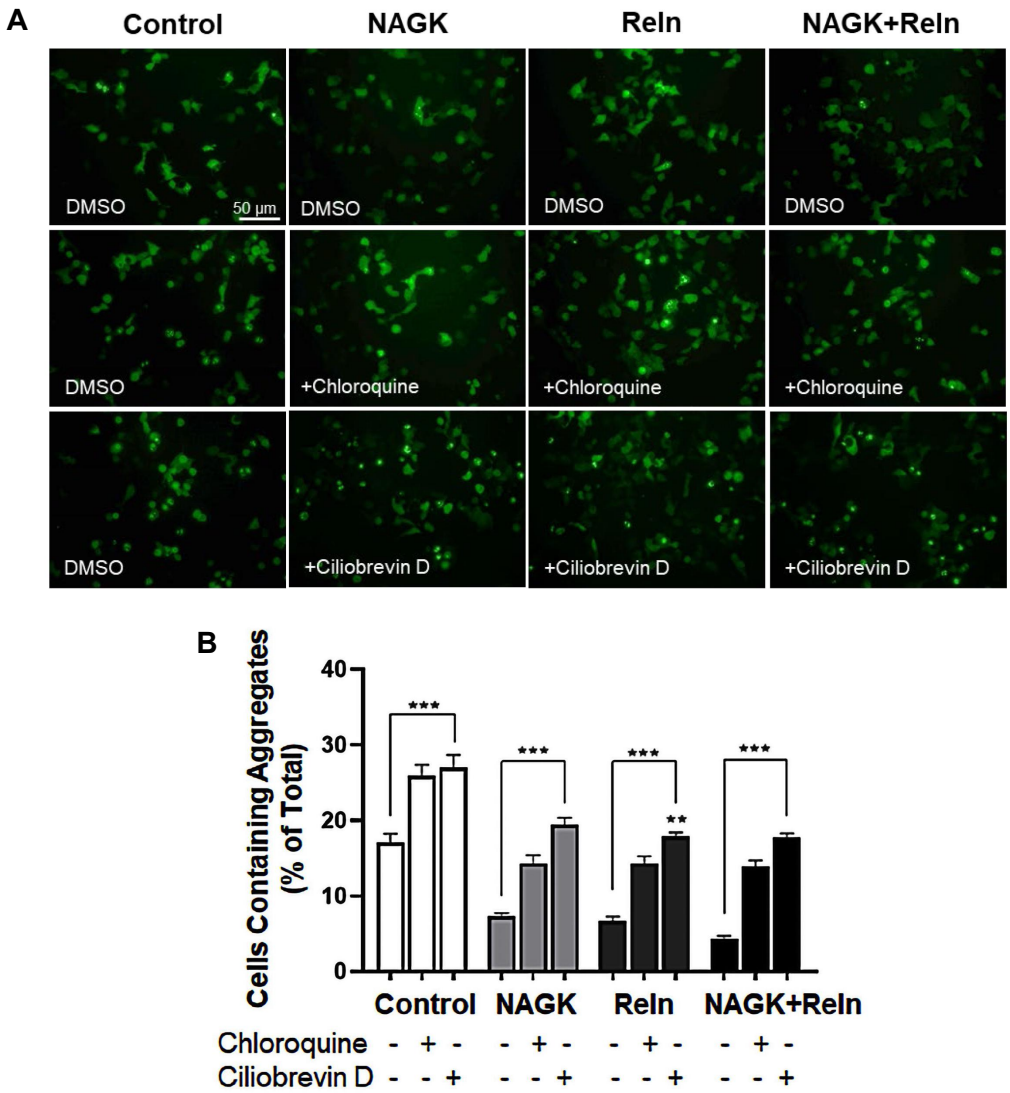

Fig. 5. Inhibition of dynein or autophagy reverses the effects of *NAGK* and *Reln* CAS activated decreases of Q74 aggregation. HEK293T cells were transfected with pQ74 and single or combined *NAGK* and *Reln* CAS plasmids. After 6 hr of transfection. Cells were treated with chloroquine (50 μM) or ciliobrevin D (20 μM) for 24 h. (A) Typical live cell images. (B) Portions of aggregate containing cells were (n=500) and expressed as mean ± SD. Statistical significance was determined using one-way ANOVA $^{**}p<0.01$, $^{***}p<0.001$. Scale bar, 50 μm.

mic aggregates.

Previous reports from our laboratory showed that NAGK upregulated dynein's function in aggregate clearance [39], migration [18] and neuritogenesis [19, 20, 25]. Interestingly, the upregulation of dynein function by NAGK was not NAGK's enzyme activity by a structural role [25, 26]. Later, we found NAGK interacted with the Roadblock-1 subunit of dynein [19, 39], indicating that dynein activation by NAGK is due to a structural interaction between the two proteins.

The large extracellular matrix glycoprotein R [7] regulates neurodevelopment and has been implicated in neurological diseases [5, 42]. Binding of Cajal-Retzius cell-secreted Reln lipoprotein receptors triggers a cascade of events resulting in the activation of kinases that modulate MTs during neuronal migration and hippocampal dendrite development [5, 12, 17, 24, 43]. Reln, a secreted glycoprotein controlling neuronal positioning, functions by clustering its receptors VLDLR and ApoER2, causing the activation of src-family kinases (SRKs) and the phosphorylation of the adapter molecule Dab1 (reviewed by [43]). The phosphorylated Dab1 recruits Lis1 [1], which regulates the function of cytoplasmic dynein/dynactin motor complex [10, 30, 41, 47].

Cytoplasmic dyneins play a crucial role in clearing protein aggregates, by retrogradely transporting aggregates to MTOC

for lysosomal degradation. In this study, we employed the CRISPR/dCas9 activation system (CAS) to activate *NAGK* and *Reln* genes, which in turn promote dynein-mediated autophagy. In conclusion, the present study provides evidence for the improvement of cell health by efficient clearance of mHtt through CAS activation of *NAGK* and *Reln* genes.

Acknowledgments

The study was supported by the Basic Science Research Program through the National Research Foundation of Korea (NRF) (grant no. NRF-2022R1A6A3A01087627 to H.J.C. and NRF-2021R1A2C1008564 to I.S.M.).

The Conflict of Interest Statement

The authors declare that they have no conflicts of interest with the contents of this article.

Reference

1. Assadi, A. H., Zhang, G., Beffert, U., McNeil, R. S., Renfro, A. L., Niu, S., Quattrocchi, C. C., Antalffy, B. A., Sheldon, M., Armstrong, D. D. and Wynshaw-Boris, A. 2003. Interaction of reelin signaling and Lis1 in brain development. *Nat. Genet.* **35,** 270-276.
2. Bence, N. F., Sampat, R. M. and Kopito, R. R. 2001. Impairment of the ubiquitin-proteasome system by protein aggregation. *Science* **292**, 1552-1555.
3. Bjorkoy, G., Lamark, T., Brech, A., Outzen, H., Perander, M., Overvatn, A., Stenmark, H. and Johansen, T. 2005. p62/SQSTM1 forms protein aggregates degraded by autophagy and has a protective effect on huntingtin-induced cell death. *J. Cell Biol.* **171**, 603-614.
4. Brewer, G. J., Torricelli, J. R., Evege, E. K. and Price, P. J. 1993. Optimized survival of hippocampal neurons in B27-supplemented neurobasal™, a new serum-free medium combination. *J. Neurosci. Res.* **35**, 567-576.
5. Chai, X., Förster, E., Zhao, S., Bock, H. H. and Frotscher, M. 2009. Reelin stabilizes the actin cytoskeleton of neuronal processes by inducing n-cofilin phosphorylation at serine3. *J. Neurosci. Res.* **29**, 288-299.
6. Chin, L. S., Olzmann, J. A. and Li, L. 2010. Parkin-mediated ubiquitin signalling in aggresome formation and autophagy. *Biochem. Soc. Trans.* **38**, 144-149.
7. D'Arcangelo, G., Nakajima, K., Miyata, T., Ogawa, M., Mikoshiba, K. and Curran, T. 1997. Reelin is a secreted glycoprotein recognized by the CR-50 monoclonal antibody. *J. Neurosci. Res.* **17**, 23-31.
8. Duyao, M. P., Ambrose, C. M., Myers, R. H., Novelletto, A., Persichetti, F., Frontali, M., Folstein, S. E., Ross, C., Franz, M., Abbott, M. and Gray, J. 1993. Trinucleotide repeat length instability and age of onset in Huntington's disease. *Nat. Genet.* **4**, 387-392.
9. Egan, M. J., McClintock, M. A., Hollyer, I. H., Elliott, H. L. and Reck-Peterson, S. L. 2015. Cytoplasmic dynein is required for the spatial organization of protein aggregates in filamentous fungi. *Cell Rep.* **11**, 201-209.
10. Faulkner, N. E., Dujardin, D. L., Tai, C. Y., Vaughan, K. T., O'Connell, C. B., Wang, Y. L. and Vallee, R. B. 2000. A role for the lissencephaly gene LIS1 in mitosis and cytoplasmic dynein function. *Nat. Cell. Biol.* **2**, 784-791.
11. Fleming, A. and Rubinsztein, D. C. 2020. Autophagy in neuronal development and plasticity. *Trends Neurosci.* **43**, 767-779.
12. Förster, E., Tielsch, A., Saum, B., Weiss, K. H., Johanssen, C., Graus-Porta, D., Müller, U. and Frotscher, M. 2002. Reelin, Disabled 1, and beta 1 integrins are required for the formation of the radial glial scaffold in the hippocampus. *Proc. Natl. Acad. Sci. USA.* **99**, 13178-13183.
13. Fuertes, G., Martín De Llano, J. J., Villarroya, A., Rivett, A. J. and Knecht, E. 2003. Changes in the proteolytic activities of proteasomes and lysosomes in human fibroblasts produced by serum withdrawal, amino-acid deprivation and confluent conditions. *Biochem. J.* **375**, 75-86.
14. Gao, Z. and Godbout, R., 2013. Reelin-Disabled-1 signaling in neuronal migration: splicing takes the stage. *Cell. Mol. Life Sci.* **70**, 2319-2329.
15. Gregersen, N. 2006. Protein misfolding disorders: Pathogenesis and intervention. *J. Inherit. Metab. Dis.* **29**, 456-470.
16. Haque, M. N. and Moon, I. S. 2020. Stigmasterol promotes neuronal migration via reelin signaling in neurosphere migration assays. *Nutr. Neurosci.* **23**, 679-687.
17. Herz, J. and Chen, Y. 2006. Reelin, lipoprotein receptors and synaptic plasticity. *Nat. Rev. Neurosci.* **7**, 850-859.
18. Islam, M. A., Choi, H. J., Dash, R., Sharif, S. R., Oktaviani, D. F., Seog, D. H. and Moon, I. S. 2020. N-acetyl-D-Glucosamine kinase interacts with NudC and Lis1 in dynein motor complex and promotes cell migration. *Int. J. Mol. Sci.* **22**, 129.
19. Islam, M. A., Sharif, S. R., Lee, H. and Moon, I. S. 2015. N-acetyl-D-glucosamine kinase promotes the axonal growth of developing neurons. *Mol. Cells* **38**, 876-885.
20. Islam, M. A., Sharif, S. R., Lee, H., Seog, D. H., Moon, I. S. 2015. N-acetyl-D-glucosamine kinase interacts with dynein light-chain roadblock type 1 at Golgi outposts in neuronal dendritic branch points. *Exp. Mol. Med.* **47**, e177-e177.
21. Johnston, J. A., Ward, C. L. and Kopito, R. R. 1998. Aggresomes: a cellular response to misfolded proteins. *J. Cell Biol.* **143**, 1883-1898.
22. Kawaguchi, Y., Kovacs, J. J., McLaurin, A., Vance, J. M., Ito, A. and Yao, T. P. 2003. The deacetylase HDAC6 regulates aggresome formation and cell viability in response to misfolded protein stress. *Cell* **115**, 727-738.
23. Kocaturk, N. M. and Gozuacik, D. 2018. Crosstalk between mammalian autophagy and the ubiquitin-proteasome system. *Front. Cell Dev. Biol.* **6**, 128.

24. Lakatosova, S. and Ostatnikova, D. 2012. Reelin and its complex involvement in brain development and function. *Int. J. Biochem. Cell Biol.* **44**, 1501-1504.
25. Lee, H., Cho, S. J. and Moon, I. S. 2014. The non-canonical effect of N-acetyl-D-glucosamine kinase on the formation of neuronal dendrites. *Mol. Cells* **37**, 248-256.
26. Lee, H., Dutta, S. and Moon, I. S. 2014. Upregulation of dendritic arborization by N-acetyl-D-glucosamine kinase is not dependent on its kinase activity. *Mol. Cells* **37**, 322-329
27. Malik, B. R., Maddison, D. C., Smith, G. A. and Peters, O. M. 2019. Autophagic and endo-lysosomal dysfunction in neurodegenerative disease. *Mol. Brain* **12**, 100.
28. Mauthe, M., Orhon, I., Rocchi, C., Zhou, X., Luhr, M., Hijlkema, K. J., Coppes, R. P., Engedal, N., Mari, M. and Reggiori, F. 2018. Chloroquine inhibits autophagic flux by decreasing autophagosome-lysosome fusion. *Autophagy* **14**, 1435-1455.
29. Mawuenyega, K. G., Sigurdson, W., Ovod, V., Munsell, L., Kasten, T., Morris, J. C., Yarasheski, K. E. and Bateman, R. J. 2010. Decreased clearance of CNS β-amyloid in Alzheimer's disease. *Science* **330**, 1774.
30. McKenney, R. J. 2020. LIS1 cracks open dynein. *Nat. Cell Biol.* **22**, 515-517.
31. Mizushima, N., Levine, B., Cuervo, A. M. and Klionsky, D. J. 2008. Autophagy fights disease through cellular self-digestion. *Nature* **451**, 1069-1075.
32. Moon, I. S., Cho, S. J., Jin, I. and Walikonis, R. 2007. Simple method for combined fluorescence *in situ* hybridization and immunocytochemistry. *Mol. Cells* **24**, 76-82.
33. Narain, Y., Wyttenbach, A., Rankin, J., Furlong, R. A. and Rubinsztein, D. C. 1999. A molecular investigation of true dominance in Huntington's disease. *J. Med. Genet.* **36**, 739-746.
34. Niethammer, M., Smith, D. S., Ayala, R., Peng, J., Ko, J., Lee, M. S., Morabito, M. and Tsai, L. H. 2000. NUDEL is a novel Cdk5 substrate that associates with LIS1 and cytoplasmic dynein. *Neuron* **28**, 697-711.
35. Øverbye, A., Brinchmann, M. F. and Seglen, P. O. 2007. Proteomic analysis of membrane-associated proteins from rat liver autophagosomes. *Autophagy* **3**, 300-322.
36. Park, J. J., Dempewolf, E., Zhang, W. and Wang, Z. Y. 2017. RNA-guided transcriptional activation via CRISPR/dCas9 mimics overexpression phenotypes in Arabidopsis. *PLoS One* **12**, e0179410.
37. Perez-Pinera, P., Ousterout, D. G., Brunger, J. M., Farin, A. M., Glass, K. A., Guilak, F., Crawford, G. E., Hartemink, A. J. and Gersbach, C. A. 2013. Synergistic and tunable human gene activation by combinations of synthetic transcription factors. *Nat. Methods* **10**, 239-242.
38. Ripon, M. K. H., Lee, H., Dash, R., Choi, H. J., Oktaviani, D. F., Moon, I. S. and Haque, M. N. 2020. N-acetyl-D-glucosamine kinase binds dynein light chain roadblock 1 and promotes protein aggregate clearance. *Cell Death Dis.* **11**, 619.
39. Schindelin, J., Arganda-Carreras, I., Frise, E., Kaynig, V., Longair, M., Pietzsch, T., Preibisch, S., Rueden, C., Saalfeld, S., Schmid, B., Tinevez, J. Y., White, D. J., Hartenstein, V., Eliceiri, K., Tomancak, P. and Cardona, A. 2012. Fiji: An open-source platform for biological-image analysis. *Nat. Methods* **9**, 676-682.
40. Sharif, S. R., Islam, A. and Moon, I. S. 2016. N-acetyl-D-glucosamine kinase interacts with dynein-Lis1-NudE1 complex and regulates cell division. *Mol. Cells* **39**, 669-679.
41. Smith, D. S., Niethammer, M., Ayala, R., Zhou, Y., Gambello, M. J., Wynshaw-Boris, A. and Tsai, L. H. 2000. Regulation of cytoplasmic dynein behaviour and microtubule organization by mammalian Lis1. *Nat. Cell Biol.* **2**, 767-775.
42. Stranahan, A. M., Erion, J. R. and Wosiski-Kuhn, M. 2013. Reelin signaling in development, maintenance, and plasticity of neural networks. *Ageing Res. Rev.* **12**, 815-822.
43. Tissir, F. and Goffinet, A. M. 2003. Reelin and brain development. *Nat. Rev. Neurosci.* **4**, 496-505.
44. Vallee, R. B. and Tsai, J. W. 2006. The cellular roles of the lissencephaly gene LIS1, and what they tell us about brain development. *Genes Dev.* **20**, 1384-1393.
45. Vonsattel, J. P. G., Keller, C. and Ramirez, E. P. C. 2011. Chapter 4-Huntington's disease－neuropathology. *Handb. Clin. Neurol.* **100**, 83-100.
46. Xie, R., Nguyen, S., McKeehan, W. L. and Liu, L. 2010. Acetylated microtubules are required for fusion of autophagosomes with lysosomes. *BMC Cell Biol.* **11**, 1-12.
47. Zhang, G., Assadi, A. H., McNeil, R. S., Beffert, U., Wynshaw-Boris, A., Herz, J., Clark, G. D. and D'Arcangelo, G. 2007. The Pafah1b complex interacts with the reelin receptor VLDLR. *PLoS One* **2**, e252.

초록 : CRISPR/dCas9을 통한 *NAGK* 및 *Reln* 유전자 활성화에 의한 헌팅턴병 모델에서 단백질 응집체 제거 촉진

옥타비아니 디야 파티마[1] · 다시 라주[1,2] · 하비바 사르민 움메이[1] · 최호진[1,3] · 문니 야스민 악타[1] · 석대현[4] · 메이니타 마리아 디야 누[5] · 문일수[1]*

([1]동국대학교 의과대학 해부학교실, [2]대구경북과학기술원 신생물학과, [3]동국대학교 의학연구소, [4]인제대학교 의과대학 생화학교실, [5]젠더럴 소에디르만 대학교 수산해양학부)

신경퇴행성 질환은 신경세포 내 유독한 잘못 접힌 단백질의 축적으로 특징지어진다. 따라서 효과적인 예방 및 응집체 제거를 위한 전략이 치료에 중요하다. 세포질 다이네인(dynein)은 응집체를 세포 중심으로 운반하여 용해소체(lysosome)를 통해 자가포식 분해를 진행함으로써 응집체 제거에 중요한 역할을 한다. 이전 연구에서 우리는 *N*-아세틸글루코사민 키나제(NAGK)와 Reln에 의한 다이네인의 활성화 증거를 보고했다. 본 연구에서는 NAGK와 Reln의 발현 증가가 응집체 제거에 미치는 영향을 탐구했다. HEK293T 세포(인간 배아 신장 세포주)에서 NAGK와 Reln 유전자를 발현을 촉진시키기 위해 CRISPR/dCas9 활성화 시스템(CAS)을 사용하여 표적 특이적 20 nt 가이드 RNA를 인코딩하는 특정 플라스미드를 이용했다. 이러한 유전자 표현 촉진의 효과를 돌연변이 헌팅틴(mHtt, Q74) 응집체가 유도된 헌팅턴병 세포 모델인 HEK293T 세포와 일차 마우스 피질 신경세포에서 분석했다. 결과는 NAGK 또는 Reln, 혹은 이들의 조합에 의한 CAS 활성화가 Q74 응집체('응집체')를 가진 세포의 비율을 유의미하게 감소시켰음을 보여주었다. 이 효과는 다이네인 억제제 Ciliobrevin D와 자가포식 억제제 Chloroquine에 의해 반전되었다. 이는 다이네인 매개 자가포식이 응집체 제거에 역할을 함을 나타낸다. 이러한 발견은 표적 유전자 활성화를 통해 신경세포 건강을 증진시키기 위한 치료 전략의 기초를 제공한다.